Int. J. Electrochem. Sci., 14 **(2019)** 943 – 956, doi: 10.20964/2019.01.72

International Journal of
ELECTROCHEMICAL
SCIENCE
www.electrochemsci.org

Electrochemical Sensor based on Polyethyleneimine-AuNPs-Anthraquinone-2-carboxylic acid Nanocomposite for Cysteine Detection

Manman Li[1], *Zhuangzhuang Guo*[1], *Huaixia Yang*[1], *Yanju Liu*[1,*], *Yan Tong*[1], *Jinming Kong*[2,*]

[1] Pharmacy College, Henan University of Chinese Medicine, Zhengzhou 450008, P. R. China.
[2] School of Environmental and Biological Engineering, Nanjing University of Science and Technology, Nanjing 210094, P. R. China.
[*]E-mail: liuyanju886@hactcm.edu.cn, j.kong@njust.edu.cn

Received: 30 September 2018 / *Accepted:* 6 November 2018 / *Published:* 30 November 2018

A novel electrochemical cysteine (Cys) sensing strategy based on the modification of glassy carbon electrodes with nanocomposite is presented in this paper. This proposed sensor exhibits excellent sensitivity and high selectivity toward Cys with a detection limit of 1.873×10^{-6} M. Features of the modified electrode were characterized by ultraviolet spectrophotometry (UV), contact angle (CA), transmission electron microscopy (TEM) and cyclic voltammetry (CV) methods. The reaction mechanism was explored by density functional theory, results suggested that the interaction forces between anthraquinone-2-carboxylic acid (AQCA) and Cys were hydrogen bond. Furthermore, this sensor successfully detected Cys in human serum samples with satisfactory recovery ranges, indicating a promising application in biological samples analysis and clinical diagnosis.

Keywords: Gold nanoparticle; Polyethyleneimine; Anthraquinone-2-carboxylic acid; Cysteine; electrochemical sensing

1. INTRODUCTION

Cysteine (Cys) is an essential substance in biological systems which takes part in various physiological processes [1-2]. In the process of protein folding, Cys residues thiol can stabilize protein conformation by forming disulfide bonds [3-4]. Cys can maintain the activity of some enzymes since Cys thiol group constitutes the active center of these enzymes [5-6]. It also can promote the liver's phospholipid metabolism and the recovery of liver function [7-8]. In human serum, the concentration of Cys ranges from 240 to 450 μM, its fluctuations are associated with neurotoxicity, slow growth,

hematopoietic dysfunction, liver damage and other diseases [9-11]. Therefore, the detection of Cys is of great medical significance.

Numerous methods have been developed to detect Cys, such as high-performance liquid chromatography (HPLC) [12-13], ultraviolet visible spectrometry (UV) [14-15], fluorescence spectrometry [16-18] and electrochemical method [19-20]. Among them, electrochemical method is favored due to its advantages of rapid response, high sensitivity, simple operation and low cost.

Recently, nanomaterials have been widely used in electrochemical detection [21-22], among them, gold nanoparticles (AuNPs) have been widely used owing to its good conductivity and catalytic property [23-28]. Moreover, chemical modification of its surface provides an effective attachment platform for immobilization of molecules [29]. In this proposed approach, along with promoting electrons transfer, AuNPs also serves as an efficient catalyst for one-pot formation of amide bonds between polyethyleneimine (PEI) and AQCA [30]. PEI is a water-soluble polymer in which a large amount of amine groups making it a reducing agent as well as a stabilizer for the formation of AuNPs. PEI can prevent the aggregation of nanoparticles effectively and make AuNPs stable in solution [31-32].

In this work, we synthesized PEI-AuNPs-AQCA nanocomposite and successfully fabricated an electrochemical sensor for the detection of Cys. Those results showed that the sensor had low detection limit, high selectivity and fine stability for Cys. The reaction mechanism was explored and density functional theory (DFT) results revealed that two types of hydrogen bonds were formed between AQCA and Cys. In human serum samples, it was used to detect Cys and recovery was in the range of 95.78%-104.60%, indicting a great potential prospect in biological samples analysis and clinical diagnosis.

2. MATERIAL AND METHODS

2.1 Reagents and Materials

PEI (branched, average Mw~25kDa) was purchased from Sigma-Aldrich (St. Louis, MO), $HAuCl_4 \cdot 3H_2O$ was purchased from Energy Chemical (Shang Hai, China). AQCA, Cys, alanine (Ala), phenylalanine (Phe), lysine (Lys), serine (Ser), glycine (Gly), proline (Pro) and argnine (Arg) were all purchased from J & K Scientific Ltd. (Shanghai, China). Various pH phosphate buffer saline (PBS) were prepared by mixing of appropriate amount of NaH_2PO_4, Na_2HPO_4 and KCl solutions. All other chemicals were of analytical reagent grade and used as received. Ultrapure water (≥18.25 MΩ·cm) was used throughout the experiment.

2.2 Apparatus

UV-vis absorption spectra were collected by UV-2600 (Techcomp, China). The diameter of AuNPs was determined by a ZEN5600 nanoparticle analyzer (Malvern, UK). Transmission electron microscopy (TEM) image was obtained with a HT7700 transmission electron microscope (Hitachi, Japan). The water contact angle was measured by Drop Shape Analyzer-DSA100 instrument (KRUSS, Germany). Electrochemical experiments were carried out on a RST5200F electrochemical workstation

(Shiruisi, China) with a three-electrode system consisting of a glassy carbon electrode (GCE, 3mm in diameter), a saturated calomel electrode, a platinum wire (Shiruisi, China) as working, reference and counter electrodes, respectively.

2.3 Synthesis of PEI-AuNPs

According to the reports of Brondani [33] and Kong [30, 34], the PEI-AuNPs was synthesized. Firstly, the glassware and magnet were soaked in aqua regia overnight, then washed with ultrapure water and dried. Secondly, the PEI of 2.060 g was added to 20 ml of 1.0 mM $HAuCl_4$ solution and stirred well, then heated to 80 ºC at a rate of 5 ºC·min^{-1} until the solution appeared light ruby red and cooled to room temperature.

2.4 Synthesis of PEI-AuNPs-AQCA composite

2.0 mL PEI-AuNPs solution prepared in the previous step was added to 4.8 mL of 1.0 mM AQCA solution (Fig. 1a). After stirring for 1.0 h at room temperature, the mixture was centrifuged at 14,000 rpm for 80 minutes to remove the supernatant. Then it was centrifuged again for 40 minutes. After removal of the supernatant, the resulting precipitate was redispersed in methanol and stored at 4 ºC.

2.5 Preparation of electrochemical biosensor

Prior to use, the GCE was polished to obtain a mirror surface on a polishing board containing 0.05 μm alumina powder suspension, then rinsed with ultrapure water and tested by CV in a potassium ferricyanide electrolytic solution, the redox peak potential difference of the polished GCE should be less than 80 mV. Then it was ultrasonically washed with ethanol and ultrapure water for 2 min respectively and dried with nitrogen. The cleaned electrode was modified with the as-prepared PEI-AuNPs-AQCA nanocomposite by drop coating method and dried under vacuum, the preparation steps are illustrated in Fig. 1b.

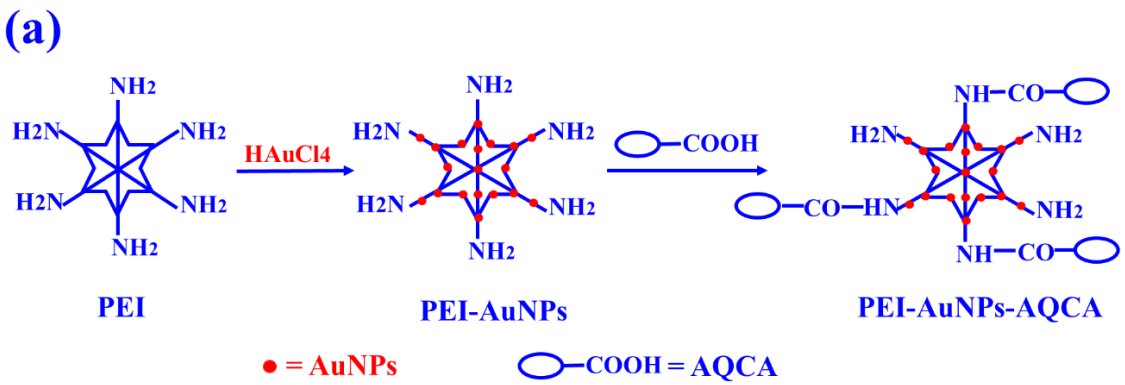

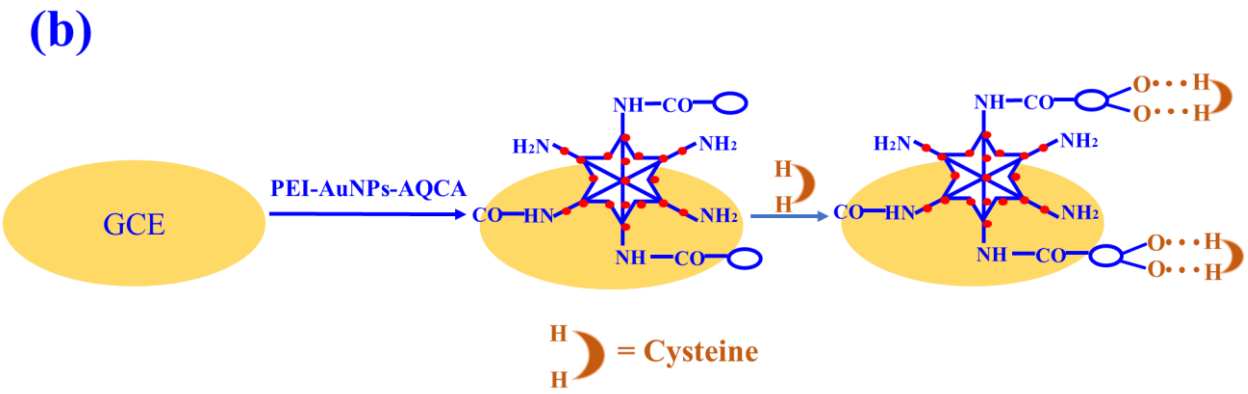

Figure 1. (a) Synthetic schematic diagram of PEI-AuNPs-AQCA nanocomposite. (b) Schematic illustration of the fabrication of the proposed electrochemical cysteine biosensor.

2.6 Electrochemical measurements

DPV curves of different electrodes (bare/PEI-AuNPs/PEI-AuNPs-AQCA) were measured by a RST5200F electrochemical workstation. Electrolyte solution contained PBS (0.10 mM, pH 7.0) and KCl (0.10 mM). CV curves of PEI-AuNPs-AQCA nanocomposite modified electrode were tested at different scan rates (0.01-0.30 V s^{-1}), different pH values (6.0, 6.5, 7.0, 7.5, 8.0) and different modification amounts (1, 2, 3, 4, 5, 6 μL) at the presence of 0.40 mM Cys. Under optimized experimental conditions, DPV method was selected to investigate the responses of the as-prepared sensor toward various concentrations of Cys, the linear relationship was plotted. DPV (scanning range 0.1-1.0 V, increment 0.004 V) method was used in interference, stability, reproducibility study and real samples analysis as well.

2.7 Theoretical calculations

The reaction mechanism between AQCA and Cys was explored by density functional theory, the ground state structures of molecules were optimized and the single point energies were calculated at the level of PBEPBE/6-31+G (d). All the calculations were conducted by Gaussian09 program package.

3. RESULTS AND DISCUSSION

3.1 Characterizations of materials

3.1.1 UV-vis absorption spectra of materials

The as-prepared PEI-AuNPs and PEI-AuNPs-AQCA nanocomposite were characterized by UV-vis absorption spectra, results were shown in Fig. 2. The absorption peaks at 324 nm and 525 nm belong to PEI and AuNPs respectively [34-35]. The solution of AQCA has a strong absorption peak at 325 nm, while the absorption of PEI-AuNPs-AQCA was 337 nm, after the interaction of PEI-AuNPs and AQCA,

amide bond was formed and a more extensive conjugate system was generated, as a result, the energy of this system decreased and a red shift of 12 nm occurred in the UV-vis absorption spectra [36].

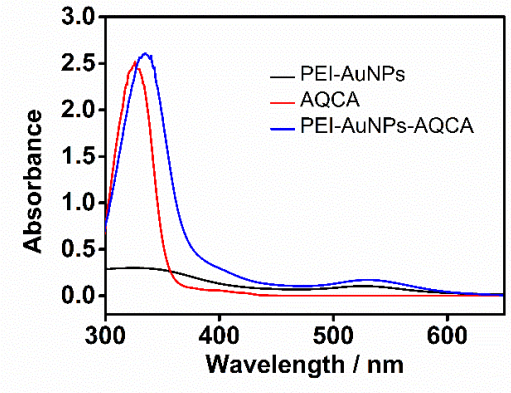

Figure 2. UV-vis absorption spectra of PEI-AuNPs, AQCA and PEI-AuNPs AQCA nanocomposite.

3.1.2 TEM Characterization

The diameter of PEI-AuNPs was measured by a nanoparticle analyzer and their average diameter was 11 nm. The morphology of PEI-AuNPs and PEI-AuNPs-AQCA were observed by transmission electron microscopy (TEM) and shown in Fig.3. The shape of gold nanoparticles was approximately spherical and uniformly dispersed in solution, which proved that PEI can maintain the dispersed state of gold nanoparticles effectively. From Fig.3 (a) it can be seen that the diameter of nanoparticles was about 10 nm, which was consistent with the result tested with the nanoparticle analyzer. Compared with Fig.3 (a), PEI-AuNPs-AQCA particles in Fig.3 (b) became slightly larger than that of the particles without AQCA. The TEM images showed that the nanocomposites were synthesized successfully.

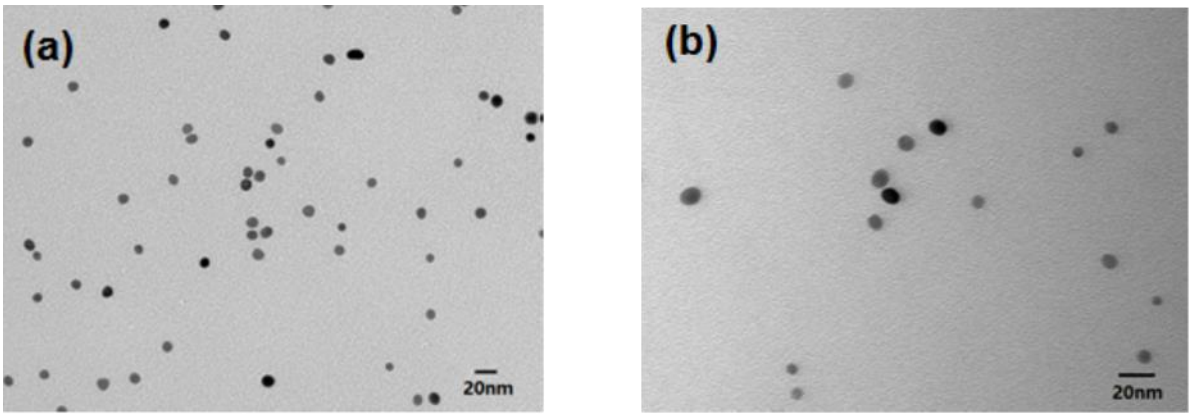

Figure 3. TEM image of (a) PEI-AuNPs, (b) PEI-AuNPs-AQCA nanocomposite.

3.1.3 Contact angle

Water contact angle (WCA) helps to analyze the surface property of different material. The variation of WCA of different electrodes were shown in Fig. 4. After modifying PEI-AuNPs, the surface of the electrode formed a cambered surface and the contact angel (60.9°) was smaller than that of the

bare electrode (71.9°), which was attributed to the abundant amine groups with low surface tension. When the electrode was modified with PEI-AuNPs-AQCA nanocomposite, compared with the electrode modified with PEI-AuNPs, the WCA was slightly increased to 65.0° due to the high surface tension of anthraquinone group. While compared with bare electrode, the WCA decreased, revealed that PEI-AuNPs-AQCA nanocomposite is more hydrophilic and has better compatibility with water, which enables the nanocomposite to be used in body fluids or other biological samples. In addition, the results of different contact angles indicated that the nanomaterials had been synthesized as designed.

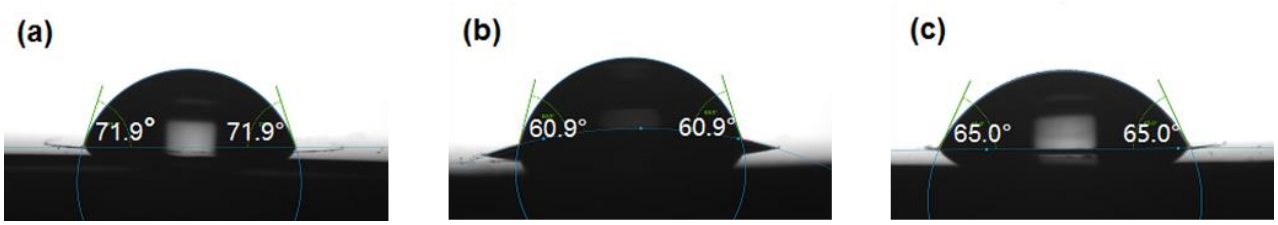

Figure 4. Water droplet on (a) bare electrode, (b) PEI-AuNPs modified electrode, (c) PEI-AuNPs-AQCA nanocomposite modified electrode.

3.2 Feasibility analysis

In order to verify the feasibility of this strategy, the responses of different electrodes (bare/PEI-AuNPs/PEI-AuNPs-AQCA) toward Cys were explored. DPV method was adopted for electrochemical testing and results were shown in Fig. 5. From the diagram it can be seen that when 0.40 mM Cys was added to the 0.10 M PBS solution, there was no electrochemical signal produced on bare electrode. A weak current signal occurred near 0.54 V when the PEI-AuNPs modified electrode was tested. When the electrode modified with PEI-AuNPs-AQCA nanocomposite was used to detect Cys, a strong electrochemical signal at 0.54 V appeared, indicating that the sensor had a significant response to Cys. The calculation results of natural bond orbit charge and single point energy suggested that two types of hydrogen bond were formed between PEI-AuNPs-AQCA and Cys, the electron cloud density of AQCA increased, made it easier for AQCA to transfer electrons with hydrogen ions. At the same time, the gold nanoparticles could promote the electrons transfer, which was beneficial to the enhancement of electrochemical signal [37-38].

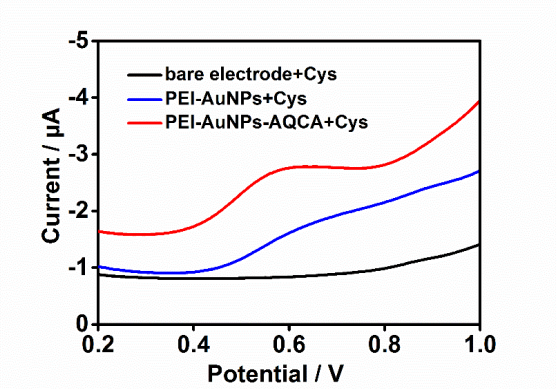

Figure 5. DPV responses of bare/PEI-AuNPs/PEI-AuNPs-AQCA electrode toward Cys (0.4 mM) respectively. Scanning range: 0.2-1.0 V, increment: 0.004 V.

3.3 Influence of scan rate

The responses of PEI-AuNPs-AQCA nanocomposite modified electrode in 0.10 M PBS containing 0.40 mM Cys at different scan rates were explored by CV method. From Fig.6 it can be seen that the current response enhanced with the increase of scan rate. The peak current intensity was linearly related to scan rate in the range of 0.01-0.30 V s^{-1} and the regression equation was I (μA) = 33.7764 v (V s^{-1}) + 3.4333 (R^2 = 0.9983), suggesting a surface-controlled electrochemical process [39-40], this was consistent with the theoretical calculations, the surface-modified nanocomposite interacted with Cys and intermolecular hydrogen bonds were formed.

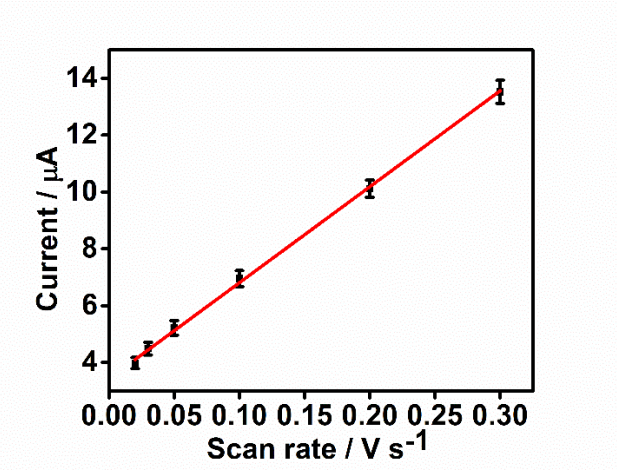

Figure 6. Change of peak current intensity *vs.* different scan rates, pH 7.0, scanning range: -0.5-1.2 V.

3.4 Optimization of experimental conditions

The electrochemical method is extremely sensitive and pH is an important factor for electrochemical sensing. In this work, CV method was used to investigate the detection of Cys with different pH values (pH = 6.0, 6.5, 7.0, 7.5, 8.0). As shown in Fig.7 (a), when the pH of electrolyte solution was in the range of 6.0-7.0, peak current intensity increased significantly, reached the maximum value when 0.40 mM Cys was added to the solution at pH of 7.0, then the peak current intensity decreased with the pH increasing. Therefore, the optimal pH of PBS buffer solution was 7.0.

Appropriate modification density is conducive to electrochemical sensing, the influence of different modification amounts (1, 2, 3, 4, 5 and 6 μL) was evaluated by CV method. As shown in Fig.7 (b), the current response toward 0.4 mM Cys enhanced obviously with the increase of the modification amount, reached the maximum when the surface modification amount was 3 μL, then peak current intensity decreased with the increasing modification amount. When the volume of the modified nanocomposite was small, the amount of nanocomposite was not enough to detect Cys, while when the modification amount was too large, it would result in the reduced conductivity [41-42], so the volume of 3 μL was selected.

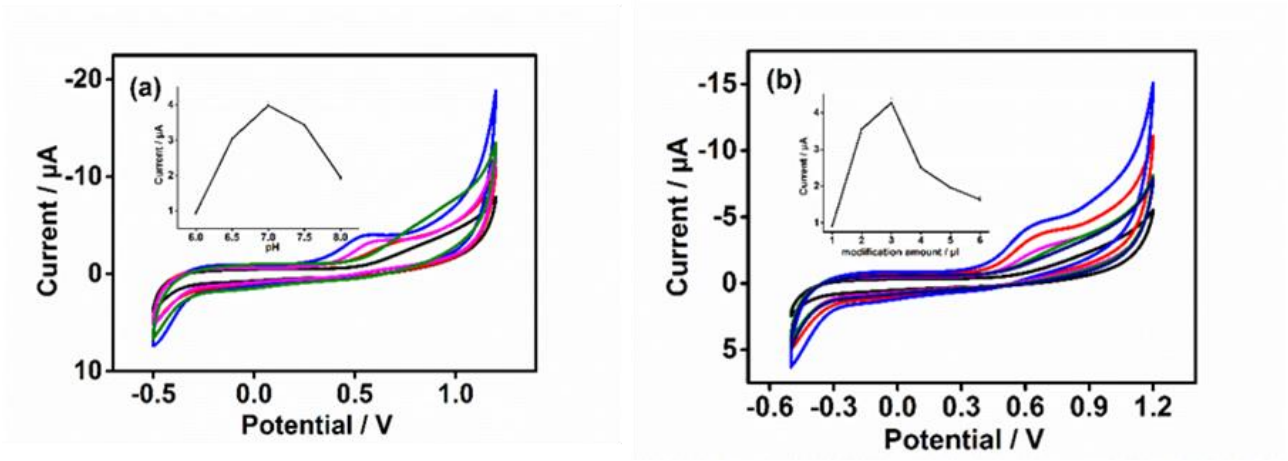

Figure 7. (a) CVs of PEI-AuNPs-AQCA nanocomposite modified electrode in 0.10 M PBS buffer solutions containing 0.40 mM Cys with (a) different pH values, (inset) changes of peak current intensity at 0.54V *vs*. different pH values; (b) different modification amounts, (inset) changes of peak current intensity at 0.54V *vs*. different modification amounts of nanocomposite. Scan rate: 0.05 V s^{-1}, scanning range: -0.5-1.2 V.

3.5 Determination of Cysteine

Under optimized conditions, the detection of Cys by as-prepared sensor was carried out using DPV method. In the Fig. 8, a significant signal peak appeared at 0.54 V with increasing Cys concentration and the peak current intensity showed a linear response in the range of 0.015-0.500 mM, with an equation I (μA) = 6.3369c (mM) + 0.8824, R^2 = 0.9968, the detection limit was 1.873×10^{-6} M according to the formula LOD = $3S_a/b$, where S_a is the standard deviation of the response and b is the slope of the calibration curve [43].

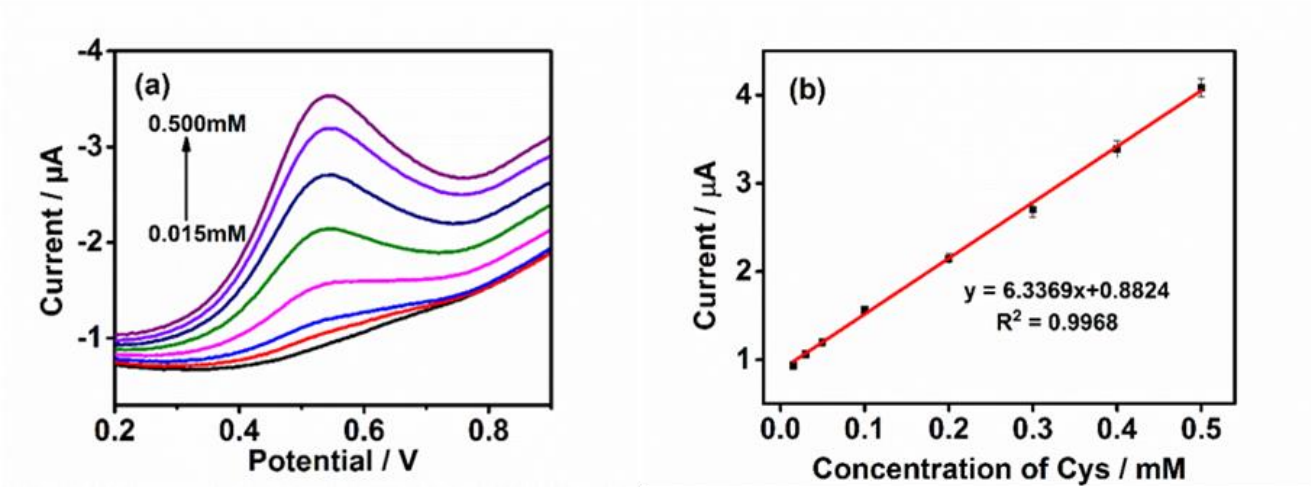

Figure 8. (a) DPV signals for 0.10 M PBS buffer solution (pH = 7.0) containing different concentrations of Cys. (b) Change of current intensity *vs*. Cys concentration (0.015-0.500 mM). Scanning range: 0.2-1.0 V, increment: 0.004 V.

Table 1. Comparison of analytical performances of some modified electrodes in the electrochemical detection of Cys

Method	Linear Range (μM)	LOD (μM)	Samples Detection	Reference
CTC/GCE	0-40	0.6	Cell tissue culture media	19
Ru-complex/CCE	5-685	1	Not given	44
AMT/GCE	20-180	3.36	Not given	45
PDMA/FMCPE	80-2250	61.7	Not given	46
[VO(Salan)] complex/CPE	240-2300	170	Not given	47
PEI-AuNPs-AQCA/GCE	15-500	1.87	Human serum	This work

CTC: cyclotricatechylene; CCE: carbon ceramic electrode; AMT: 5-amino-2-mercapto-1,3,4-thiadiazole; PDMA: poly N, N-dimethylaniline; FMCPE: Ferrocyanide film modified carbon paste electrode; CPE: carbon paste electrode.

The analytical performances of some reported electrochemical sensors used in the detection of Cys were listed in Table 1. Compared with other electrochemical sensors, the PEI-AuNPs-AQCA sensor proposed in this work showed both widely linear range and lower detection limit for the determination of Cys. In addition, it has been successfully detected Cys in human serum and expected results were obtained, indicating a great prospect in biological samples analysis and clinical diagnosis. Therefore, this novel sensor will be a powerful tool for the testing of Cys.

3.6 Reaction mechanism

The reaction mechanism between AQCA and Cys was investigated by density functional theory, results showed that two different types of hydrogen bonds N28-H41⋯O25 and S36-H38⋯O23 were formed at two different binding sites.

The ground state structures of AQCA, Cys and the interaction system of AQCA and Cys were optimized (Fig. 9). Based on the optimized structure, the natural bond orbit (NBO) charge were calculated, as shown in Table 2. After the interaction between AQCA and Cys, the charge of all atoms was changed, especially O23, O25, N28, S36, H38 and H41, indicating that the electron cloud density of these atoms changed greatly.

The calculation results revealed that the distance of H41⋯O25 was 2.18 Å and distance of H38⋯O23 was 2.27 Å, which were in accordance with the length range of hydrogen bond [48-49]. The angles of N28-H41⋯O25 and S36-H38⋯O23 were 172.17° and 165.92° respectively. To further investigate the type of interaction forces, single point energy was calculated and the interaction forces between Cys and AQCA was 21.93 kJ/mol, it was in the range of hydrogen bond energy (10-40 kJ/mol).

In short, it was postulated that hydrogen bond N28-H41⋯O25 and S36-H38⋯O23 were formed between AQCA and Cys, in which the NH⋯O=C is the most common hydrogen bonding in proteins, nucleobases and their complexes [50]. After the interaction between AQCA and Cys, the electron cloud

density of AQCA increased, which made it easier for AQCA to transfer electrons with hydrogen ions in the solution and thus a strong current signal appeared.

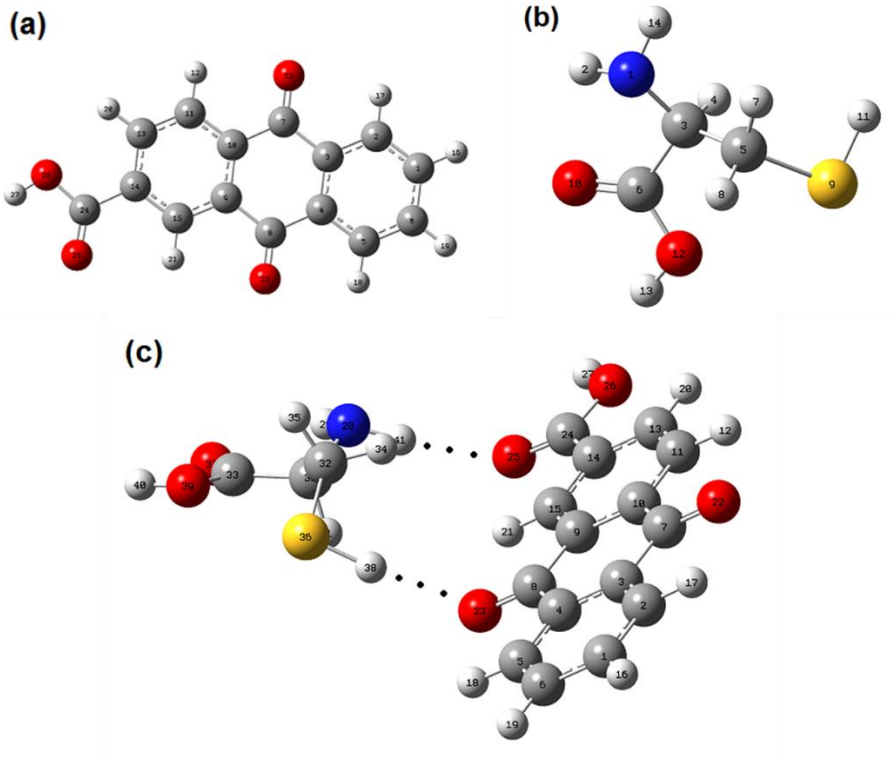

Figure 9. The optimized structure of (a) AQCA, (b) Cys, (c) the intermolecular interaction system formed by AQCQ and Cys.

Table 2. Distribution of atomic NBO charge before and after the reaction of AQCA and Cys

The atom of AQCA	The charge of atom of AQCA before reaction	The charge of atom of AQCA after reaction	Difference	The atom of Cys	The charge of atom of Cys before reaction	The charge of atom of Cys after reaction	Difference
C1	-0.225	-0.221	0.004	28N	-0.912	-0.924	-0.012
C2	-0.191	-0.190	0.001	29H	0.420	0.416	-0.004
C3	-0.119	-0.113	0.006	30C	-0.210	-0.207	0.003
C4	-0.117	-0.119	-0.002	31H	0.262	0.264	0.002
C5	-0.192	-0.188	0.004	32C	-0.630	-0.629	0.001
C6	-0.223	-0.221	0.002	33C	0.763	0.767	0.004
C7	0.513	0.501	-0.012	34H	0.275	0.271	-0.004
C8	0.512	0.520	0.008	35H	0.288	0.283	-0.005
C9	-0.109	-0.111	-0.002	36S	-0.054	-0.077	-0.023
C10	-0.101	-0.094	0.007	37O	-0.583	-0.588	-0.005
C11	-0.197	-0.194	0.003	38H	0.148	0.17	0.022
H12	0.281	0.283	0.002	39O	-0.681	-0.683	-0.002

C13	-0.188	-0.183	0.005	40H	0.517	0.513	-0.004
C14	-0.156	-0.158	-0.002	41H	0.397	0.415	0.018
C15	-0.135	-0.136	-0.001	Total	0	-0.009	-0.009
H16	0.261	0.262	0.001				
H17	0.278	0.279	0.001				
H18	0.279	0.280	0.001				
H19	0.261	0.263	0.002				
H20	0.278	0.279	0.001				
H21	0.297	0.290	-0.007				
O22	-0.510	-0.502	0.008				
O23	-0.506	-0.525	-0.019				
C24	0.741	0.753	0.012				
O25	-0.557	-0.585	-0.028				
O26	-0.695	-0.685	0.010				
H27	0.520	0.524	0.004				
Total	0	0.009	0.009				

3.7 Interference, stability and reproducibility study

To evaluate the anti-interference ability of the as-prepared sensor for Cys detection, the interference effects of non-thiol amino acid such as Ala, Phe, Lys, Ser, Gly, Pro and Arg were tested by DPV method. Amino acids of 0.50 mM were added to the 0.10 M PBS buffer solution separately, only when Cys was added, there were signal peak occurred. PEI-AuNPs-AQCA nanocomposite modified electrode did not respond to the other amino acids. The current values at 0.54 V are shown in Fig. 10 (a). When 0.50 mM any of these amino acids was added to 0.10 M PBS buffer solution containing 0.30 mM Cys, the current intensity of the modified electrode responding to Cys was almost unaffected, which indicated that the fabricated sensor has good selectivity for Cys.

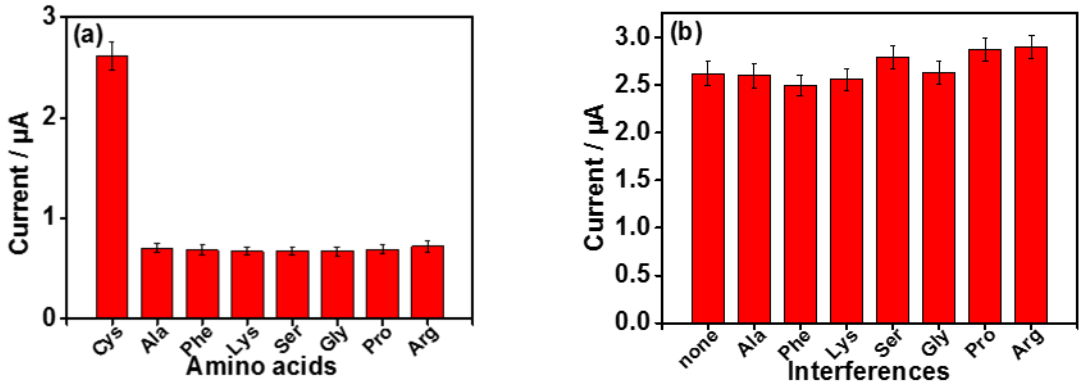

Figure 10. (a) Current intensity of the PEI-AuNPs-AQCA nanocomposite modified electrode responded to different amino acids. (b) Current intensity of the PEI-AuNPs-AQCA nanocomposite modified electrode responded to different amino acids at the present of interferences at 0.54V. Scanning range:0.2-1.0 V, increment: 0.004 V.

To estimate the stability of the as-prepared sensor, the modified electrodes were stored in a refrigerator at 4 ºC and the current response was tested at regular intervals. The current intensity was remained 92.5％ after two weeks. The reproducibility was also studied six times and the RSD of the peak currents were 3.6％, suggesting a good reproducibility.

3.8 Detection capability in serum samples

To further investigate the application of this sensor in real sample analysis, it was used to detect Cys in human serum. The human serum was diluted with 0.10 M PBS buffer solution for 20 times and 100 times and all the samples were added with Cys in different concentrations. From Table 3 it can be seen that the recovery ranges from 99.20 to 104.60%, this satisfactory result indicates that the proposed sensor can detect Cys in complicated system and it has great potential prospect in biological samples analysis and clinical diagnosis.

Table 3. Detection of Cys in diluted human serum samples (n=3)

Sample	Added(mM)	Found(mM)	Recovery (%)	RSD (%)
1% serum	0.05	0.0496	99.20	2.72
	0.50	0.5180	103.68	3.24
5% serum	0.15	0.1566	104.40	3.76
	0.30	0.3138	104.60	4.22

4. CONCLUSION

In summary, we have demonstrated the synthesis of PEI-AuNPs-AQCA nanocomposite and the glassy carbon electrode modified with this nanocomposite has a good detection effect for Cys. The proposed sensor is easy to construct and presents good characteristics such as low detention limit, high selectivity, wide linear range and fine stability. The reaction mechanism between AQCA and Cys was investigated and results indicated that two different types of hydrogen bonds were formed between the two molecules. Furthermore, the detection capability for Cys in human serum sample was tested and desired results were achieved, which promises great potential in practical applications.

ACKNOWLEDGEMENTS
This work was supported by the National Natural Science Foundation of China (grant number 21575066), Henan Province basic and frontier technology research projects (152300410214), Program for the key scientific research project of colleges and universities in Henan Province (16A350002), and Science & Technology Innovation Talents of Henan University of Chinese Medicine (2014XCXRC04). Henan University of Chinese Medicine, provincial scientific research business (2014KYYWF-QN03).

References

1. Y. Q. Tang, L. Y. Jin, B. Z. Yin, *Anal. Chim. Acta*, 993 (2017) 87.

2. H. S. Jung, X. Q. Chen, J. Kim, J. Y. Yoon, *Chem. Soc. Rev.*, 42 (2013) 6019.
3. W. R. Taylor, R E J Munro, K. Petersen, B. Robert P, *Comput. Biol. Chem.*, 27 (2003) 103.
4. G. A. Petsko, D. Ringe, Protein Structure and Function: From Sequence to Consequence, New Science Press Ltd., (2004), London, UK.
5. S. M. Marino, V. N Gladyshev, *Plos. Comput. Biol.*, 5 (2009), e1000383.
6. H. Parham, B. Zargar, *Talanta*, 65 (2005) 776.
7. M. P. Noelia, R. L. Julia, A. Nieves, *Food Chem. Toxicol.*, 114 (2018) 292.
8. E. Peixoto, C. Atorrasagasti, J. B. Aquino, R. Militello, J. Bayo, E. Fiore, F. Piccioni, E. Salvatierra, L. Alaniz, M. G. Garcia, R. Bataller, F. Corrales, M. Gidekel, O. Podhajcer, M. I. Colombo, G. Mazzolini, *Gene Ther.*, 22 (2015) 9.
9. W. W. Ma, M. Y. Wang, D. Yin, X. Zhang, *Sens. Actuators B Chem.*, 248 (2017) 332.
10. A. K. Elshorbag, V. Kozich, A. D. Smith, H. Refsum, *Curr. Opin. Clin. Nutr. Metab. Care*, 15 (2012) 49.
11. R. Janaky, V. Varga, A. Hermann, P. Saransaari, S. S. Oja, *Neurochem. Res.*, 25 (2000) 1397.
12. G. Cevasco, A. M. Piatek, C. Scapolla, S. Thea, *J. Chromatogr. A.*, 1217 (2010) 2158.
13. M. Isokawa, K. Kobayashi, Y. Miyoshi, M. Mita, T. Funatsu, K. Hamase, M. Tsunoda, *Chromatography*, 37 (2016) 147.
14. S. Mohammadi, G. Khayatian, *Spectrochim. Acta. A. Mol. Biomol. Spectrosc.*, 185 (2017) 27.
15. I. Sanskriti, K. K. Upadhyay, *ChemistrySelect*, 2 (2017) 11200.
16. G. X. Yin, T. T. Niu, Y. B. Gan, T. Yu, P. Yin, H. M. Chen, Y. Y. Zhang, H. T. Li, S. Z. Yao, *Angew. Chem. Int. Ed. Engl.*, 57 (2018) 4991.
17. L. Yang, Y. N. Su, Y. N. Geng, F. P. Qi, X. J. Ren, F. Zhang, X. Z. Song, *Anal. Chim. Acta*, 1034 (2018) 168.
18. F. Z. Chen, D. M. Han, Y. Gao, H. Liu, S. F. Wang, F. Y. Zhou, K. B. Li, S. Q. Zhang, W. J. Shao, Y. L. He, *Talanta*, 187 (2018) 19.
19. P. T. Lee, J. E. Thomson, A. Karina, C. Salter, C. Johnston, S. G. Davies, R. G. Compton, *Analyst*, 140 (2015) 236.
20. A. Nezamzadeh-Ejhieha, H. S. Hashemi, *Talanta*, 88 (2012) 201.
21. M. H. Mahmoudi, R. Zohreh, M. Asghar, A. M. Reza, M. R. Aflatoonian, *Int. J. electrochem. Sci.*, 13 (2018) 3070.
22. E. H. El-Ads, N. F. Atta, A. Galal, N. A. Eid, *Int. J. electrochem. sci.*, 13 (2018) 1452.
23. D. M. Wang, Q. Q. Gai, R. F. Huang, X. W. Zheng. *Biosens. Bioelectron*., 98 (2017) 134.
24. X. Liu, C. Fang, J. L. Yan, H. L. Li, Y. F. Tu, *Bioelectrochemistry,* 123 (2018) 211.
25. X. X. Ma, C. Fang, J. L. Yan, Q. Zhao, Y. F. Tu, *Talanta*, 186 (2018) 206.
26. X. L. Qin, C. Y. Gu, M. H. Wang, Y. F. Dong, X. Nie, M. X. Li, Z. W. Zhu, D. Yang, Y. H. Shao, *Anal. Chem.*, 90 (2018) 2826.
27. S. Y. Zhai, C. Fang, J. L. Yan, Q. Zhao, Y. F. Tu, *Anal. Chim. Acta*, 982 (2017) 62.
28. Q. Zhu, F. D. Cai, J. Zhang, K. Zhao, A. P. Deng, J. G. Li, *Biosens. Bioelectron.*, 86 (2016) 899.
29. S. A. Shahamirifard, M. Ghaedi, Z. Razmi, S. Hajati, *Biosens. Bioelectron*., 114 (2018) 30.
30. J. M. Kong, X. H. Yu, W. W. Hu, Q. Hu, S. L. Shui, L. Z. Li, X. J. Han, H. F. Xie, X. J. Zhang, T. H. Wang, *Analyst*, 140 (2015) 7792.
31. A. Koeth, J. Koetz, D. Appelhans, B. Voit, *Colloid Polym. Sci*., 286 (2008) 1317.
32. P. Veerakumar, M. Velayudham, K. L. Lu, S. Rajagopal, *Appl. Catal. A. Gen*., 455 (2013) 247.
33. D. Brondani, B. de Souza, B. S. Souza, A. Neves, I. C. Vieira, *Biosens. Bioelectron.*, 42 (2013) 242.
34. S. M. Gu, K. F. Ma, J. M. Kong, K. A. Al-Ghanim, S. Mahboob, Y. Liu, X. J. Zhang, *Int. J. electrochem. sci.*, 12 (2017) 5092.
35. W. Haiss, N. T. K. Thanh, J. Aveyard, D. G. Fernig, *Anal, Chem.*, 79 (2007) 4215.
36. J. P. Idoux, R. Zarrillo, *J. Org. Chem.*, 40 (1975) 1519.
37. M. Roushani, A. Valipour, M. Valipour, *Mater. Sci. Eng. C. Mater. Biol. Appl.*, 61 (2016) 344.

38. H. Miao, J. Yang, Y. X. Wei, W. L. Li, Y. F. Zhu, *Appl. Catal. B.*, 239 (2018) 61.
39. Y. Chen, Y. Li, D. Sun, D. B. Tian, J. R. Zhang, J. J. Zhu, *J. Mater. Chem.*, 21 (2011) 7604.
40. J. Chen, W. D. Zhang, J. S. Ye, *Electrochem. Commun.*, 10 (2008), 1268.
41. X. R. Chen, Q. Li, S. J. Yu, B. Lin, K. B. Wu, *Electrochim. Acta*, 81 (2012), 106
42. L. D. Ji, Q. Cheng, K. B. Wu, X. F. Yang, *Sens. Actuators B Chem.*, 231 (2016) 12.
43. A. Shrivastava, V. B. Gupta, *Chron. Young Sc*ientists, 2 (2011) 21.
44. A. Salimi, S. Pourbeyram, *Talanta*, 60 (2003) 205.
45. P. Kalimuthu, S. A. John, *Electrochem. Commun.*, 11 (2009) 367.
46. R. Ojani, J. B. Raoof, E. Zarei, J. Electroanal. Chem., 638 (2010) 641.
47. M. F. S. Teixeira, E. R. Dockal, E. T. G. Cavalherio, *Sens. Actuators B Chem.*, 106 (2005) 619.
48. G. Q. Wu, Inorganic Chemistry, Higher Education Press, (2002), Beijing, China.
49. Q. Li, F. Q. Huang, *Acta. Phys-chim. Sin.*, 21 (2005), 52.
50. R. P. Apaya, M. Bondi, S. L. Price, *J. Comput. Aided Mol. Des.*, 11 (1997) 479.